Transactions of the Japan Welding Society, Vol. 10, No. 2, October 1979

An Investigation of Electron Beam Welding of Sintered Iron*

By Yoshifumi SUEZAWA**, Hideo KURODA*** and Hideki KOBAYASHI***

Abstract

This report shows some experimental data concerning the electron beam welding of a sintered iron having various kinds of porosities. The purpose of this investigation is to make clear the relation between the welding conditions and the weld structure, and shrinkage of weld zone of the sintered iron. The results obtained are summarized as follows:

(1) *The pores in a sintered iron zone which the electron beam had penetrated, disappeared and the zone turned into a solid state because of the sintered structurs had been melted by the beam current. And the difference between the structure of weld zone and that of base sintered iron was clearly observed.*

(2) *It was observed that several cracks which cuased a lowering of the weld strength developed at the boundary of the weld zone owing to the high porosity of a sintered iron or passage of a high beam current.*

(3) *The penetrating depth of beam current increased with an increased beam current and an increased accelerating voltage, as well as an increased the porosity of sintered iron.*

(4) *The penetrating width of specimen increased with an increased beam current, but concerning the accelerating voltage, a reverse tendency was observed because of the electron beam diameter being pinched due to an increased accelerating voltage.*

Introduction

Recently, various kinds of sintered metal products have been used by the mechanical industries. The mechanical strength of these products are as high as those manufactured by forging or machining. But, it is very difficult to manufacture a machine part with a complicated shape by one body forming process. Such complicated machine parts have been manufactured by metallurgical process, for instance, welding, soldering or brazing.

The purpose of this study is to show clearly the joining process of sintered iron by the electron beam welding with high energy.

Experiment

There are few reports concerning the welding of sintered metals. We have only three papers on the subject by Mr. W.V. Knoop[1], Mr. J.F. Hinrich[2] and Prof. Onishi[3].

2.1 *Manufacturing of sintered metal specimens*

2.1.1 Materials

(i) Quality: Pure iron (electrolytic iron) manufactured by TOHO Zinc Co., Ltd. (MIRON-P)

(ii) Elements: Fe 99.95%, C 0.01%, P<0.01%, S<0.01% and few insoluble elements for acid

(iii) Grade: 200 mesh

2.1.2 Forming conditions

(i) Dimensions: 23.6ϕ×35 mm

(ii) Forming machine: Oil pressure forming press (capacity: 50 tons)

(iii) Forming method:
The above mentioned pure iron powder was compressed by a 50 tons oil pressure forming press in the die, being coated with Zinc-stearate [Zn-$(C_{17}H_{35}COO)_2$] diluted with benzine under 2 ton/cm^2~5 ton/cm^2 loads. The porosities of these compressed powder pieces were 10, 12, 14, 18 and 22%.

2.1.3 Sintering conditions

(i) Temperature: 1150°C

(ii) Time: 45 min kept at 1150°C

(iii) Furnace: 35 kW resistance furnace operated in H_2 atmosphere

(iv) H_2 flow rate: 6 *l*/min

2.1.4 Measurement of porosity

The porosity of these specimens was measured by the following equation

$$P=\left(1-\frac{D}{D_0}\right)\times 100$$

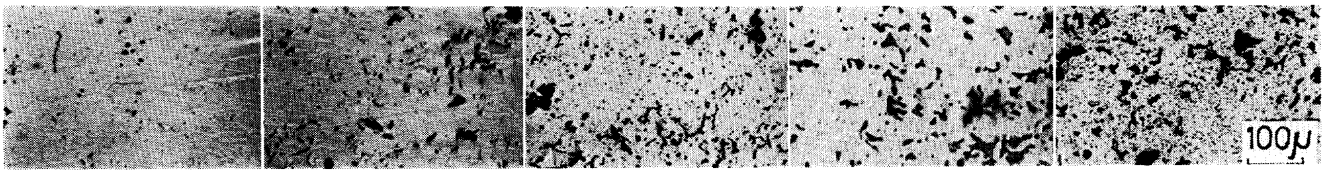

Porosity: 10% 12% 14% 18% 22%

Photo. 1 Microstructure of sintered iron

* Received 19 July 1979

** Department of Aero Space Engineering, College of Science and Technology Nihon University

*** Nippon Electric Co., Ltd.

where P : Porosity (%)
D : Density of sintered specimens (g/cm³)
D_0: Density of Fe (g/cm³)
In this experiment D_0=7.8 was used.
Photo. 1 shows the microstructure of each sintered iron having a different porosity.

2.2 *Electron beam welding of sintered iron*

After these specimens were ground and finished to 23 $\phi \times 35 \pm 0.02$ mm, their surfaces were degreased with trichloroethylene [ClCH:CCl_2] and cleaned with acetone (CH_3COOH_3) before the welding operation.

Two specimens having the same density were 3 points tack-welded on the abutted joint in longitudinal direction. And as illustrated in Fig. 1, these specimens were turned in the welding chamber by turning equipment at 600~1000 mm/min speed, and then, the electron beam was projected to the abutted joint. These operations were carried out in the vacuum chamber at 5×10^{-4} Torr. As indicated in Fig. 2(a) (center of specimen) and (b) (lower part of specimen), the focus of the beam was fixed at two positions. And also, in order to facilitate gas exhaustion from the welded zone, the welding operations were carried out using the specimens having a 3 mm diameter hole as shown in (c) (center of specimen). In the case of Fig. 2(d), a good result was not achieved because of the melting down of both sides of the specimen when the electron beam passed through.

Concerning the means of determining the focus position, there are two ways well known, one being the visual focal pointprocess, that is, a narrow beam which has a strong bright point at the beam projected position is applied on the metal surface using a weak current. The other is the AB test process proposed by Prof. Arata, that is, the actual focal point determined under practical welding conditions. In this experiment, the focus position was determined by the former

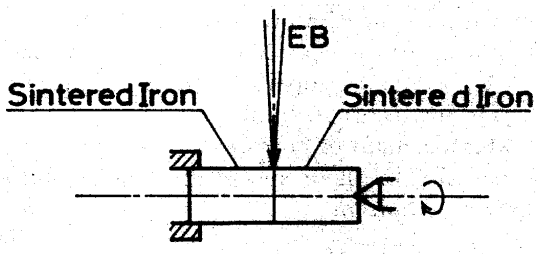

Fig. 1 Welding method

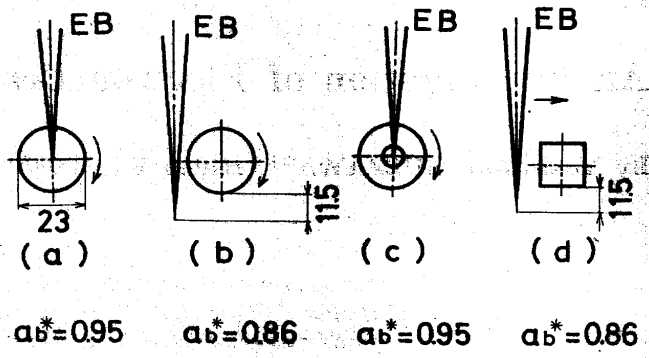

Fig. 2 Focus positions and movement of specimens

means. Also, as is well known, the effects of the focus position on the result of welding are shown by the active parameter, a_b value. In this experiment, the symbol a_b* was used to denote clearly the visual focal point. This experiment was carried out under a constant working distance. Furthermore, in order to accelerate the gas exhaustion and to prevent occurrence of pores at the welded zone, a 500 Hz, 3 mm amplitude capacity beam deflecting equipment was used. The welding conditions used in this experiment are shown in Table 1.

Results and Discussions

3.1 *Welded structure of sintered iron*

3.1.1 Fusion of sintered iron

The beam penetrated zone of the sintered structure was fused and turned into a non-sintered structure with a solid phase. The fused zone has a dendrite structure as shown in Photos. 2 and 3, because of the fast cooling effects due to the surrounding zone. These two photos show a view of the difference between the fused zone and the sintered structure of base metal. Also, it was observed that this fused structure varied with welding conditions as follows.

(i) Effect of beam current

For the case of Fig. 2 (a), the relation between the beam current and the depth of penetration is illustrated in Fig. 3 (10% porosity) and Fig. 4 (22% porosity). From these figures, it is seen that the depth of penetration is greater with an increase of the beam current (at beam power=constant). In the case of solid metal, it is well known that the depth of penetration varies linealy with the beam current, but in the case of sintered metal, as shown in Figs. 3 and 4,

Table 1 E.B. Welding conditions of sintered iron

(kV) Accelerating Voltage	(mA) Beam Current	Focus Position				(mm/min) Welding Speed	(Torr) Vacuum of Welding Chamber	500 Hz Beam Deflection Equipment
		Fig. 2						
90	4~20	(a) a_b* 0.95	(b) a_b* 0.86	(c) a_b* 0.95	(d) a_b* 0.86	600~1000	5×10^{-4}	Amplitude 3 mm used
		Fig. 2						
150	4~20	(a) a_b* 0.95	(b) a_b* 0.86	(c) a_b* 0.95	(d) a^*_b 0.86	600~1000	5×10^{-4}	Amplitude 3 mm used

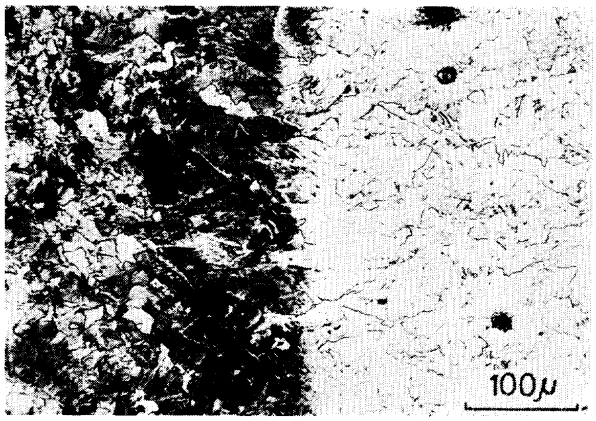

Photo. 2 Microstructure of E.B. welded sintered iron. 150 kv, 11 mA, 1000 mm/min, $a_b^*=0.95$, 18% porosity

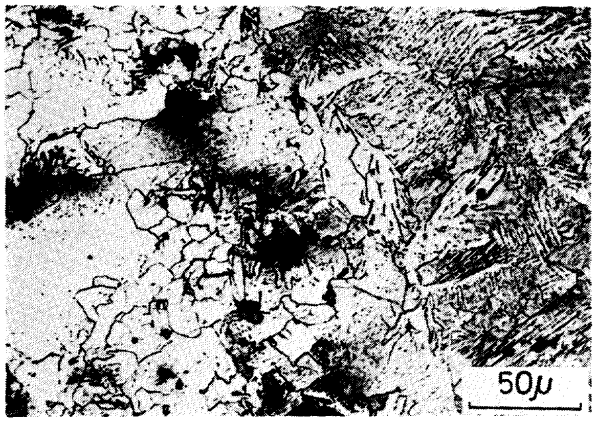

Photo. 3 Dendrite structure of E.B. welded zone. 150 kv, 11 mA, 1000 mm/min, $a_b^*=0.95$, 10% porosity

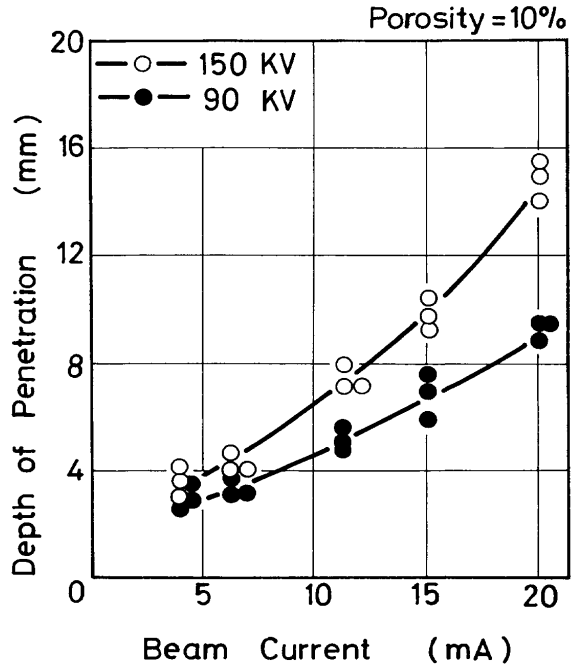

Fig. 3 Relation between beam current and depth of penetration (porosity: 10%)

it is observed that the increasing rate of the depth of penetration becomes large with an increase of the beam current, and this tendency is prominent with in-crease of the porosity as shown in Fig. 4. In the case of less than 4 mA current, as shown in Photos 4 and

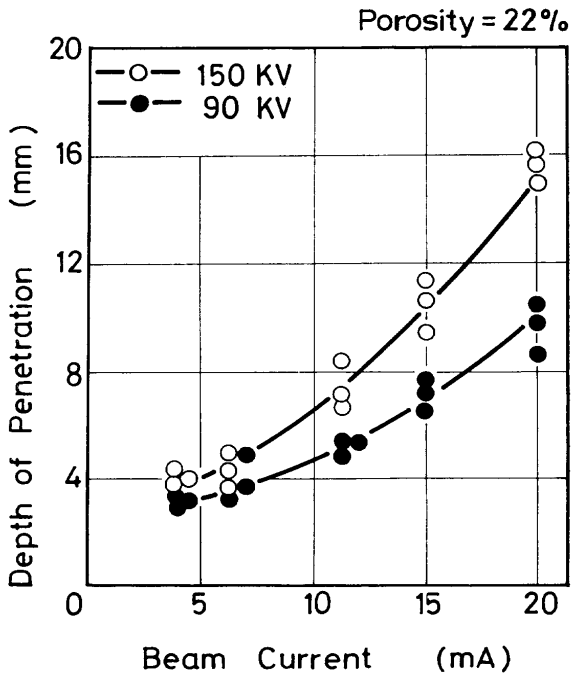

Fig. 4 Relation between beam current and depth of penetration (porosity: 22%)

Photo. 4 Penetrating depth at 4 mA, 14% porosity, 150 kv, 600 mm/min, $a_b^*=0.86$

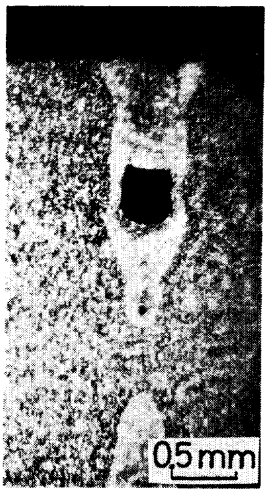

Photo. 5 Penetrating depth at 4 mA, 22% porosity, 150 kv, 1000 mm/min, $a_b^*=0.95$

5, in a few specimens there was no penetration into the center. Also, in the case of more than 15 mA beam current, there occurred some over-fused specimens with many pores. Thus, 7 mA~11 mA beam current was found the best. Photo. 6 shows the microstructure of a good welded specimen.

Concerning the width of fused zone, in a few cases it increased with an increase of beam current. From Photos. 7 and 8, it is clear that the width of the fused zone increases with an increase of the beam current. As shown in Photo. 9, in the case of specimen with high porosity, it was several times observed that a few cracks developed at the boundary zone between the fused zone and the heat affected zone. This tendency

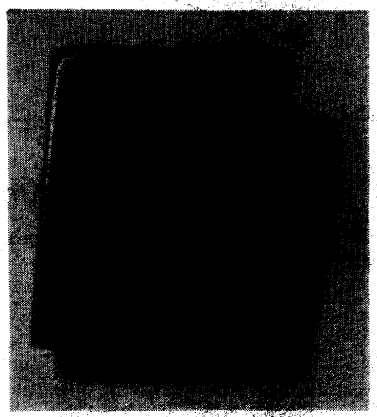

Photo. 6 View of E.B. weld of sintered iron, 150 kv, 11 mA, 1000 mm/min, $a_b^*=0.86$, 10% porosity.

Photo. 7 Wide width of E.B. welded specimen, 150 kv, 20 mA, 1000 mm/min, $a_b^*=0.86$, 22% porosity

Photo. 8 Narrow width of E.B. welded specimen, 150 kv, 11 mA, 1000 mm/min, $a_b^*=0.86$, 22% porosity

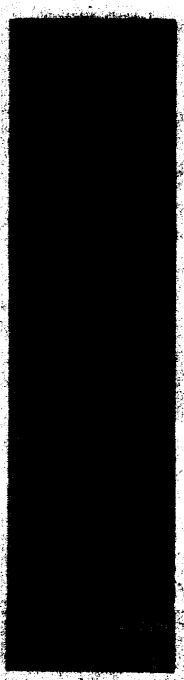

Photo. 9 View of E.B. welded structure of sintered iron, 90 kv, 20 mA, 1000 mm/min, $a_b^*=0.86$, 22% porosity

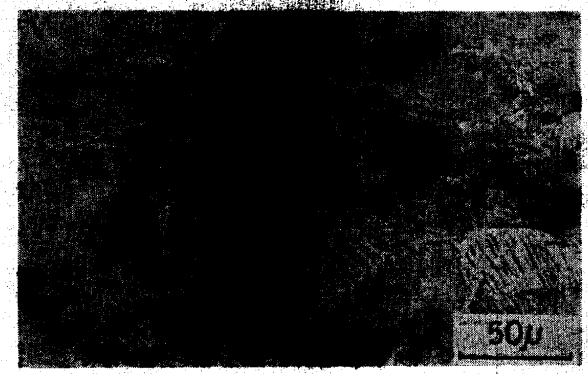

Photo. 10 View of cracks caused by E.B. welding 90 kv, 20 mA, 1000 /min, $a_b^*=0.86$, 22% porosity

increased with the beam current. Photo. 10 shows an appearance of cracks created near the fused zone, and Photo. 11 shows a good welded structure.

(ii) Effect of accelerating voltage

Concerning the relation between the accelerating voltage and the depth of penetration, as shown in Figs. 3 and 4, a large depth of penetration was obtained using a large accelrating voltage for each porosity. Photo. 9 shows the structure of a welded specimen which has not penetrated enough. Concerning the width of the fused zone, from Photos. 12 and 13, it is clear that the width of the fused zone of a specimen welded by a low accelerating voltage is greater than that of one welded by a high acclerating voltage.

3.1.2 Pores creation

(i) Pores at bead top

As shown in Photos. 4, 5 and 9, some pores were created at the top of bead as a result of penetration of the electron beam into the sintered iron which involves many pores in the structure. Concerning this phenomenon, it seems that many pores involved in the sintered iron disappeared as a result of melting the

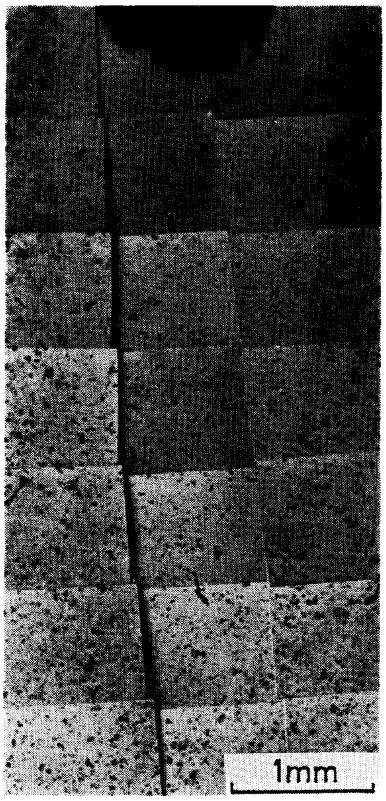

Photo. 11 View of good E.B. welded structure. 150 kv, 11 mA, 1000 mm/min, a_b*=0.86, 10% porosity

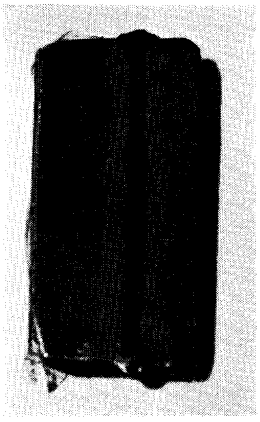

Photo. 12 View of wide width of E.B. welded specimen 90 kv, 11 mA, 1000 mm/min, a_b*=0.86, 14% Porosity

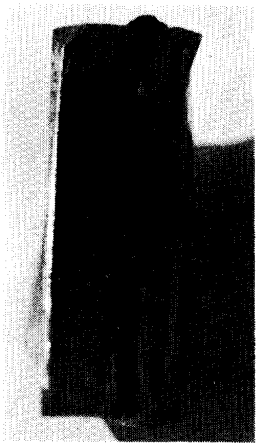

Photo. 13 View of narrow width of E.B. welded speciemn 150 kv, 11 mA, 1000 mm/min, a_b.*=0.86, 14% porosityt

sintered iron, and little inner gases were exhausted, but some of them remained in the fused metal and created porosity at the top of the bead. This porosity made a welding defect which lowered the joint strength.

(ii) Pores at the welded joint

As above mentioned, if the welding operation was carried out with pores remaining at the top of the bead and the focus position was set at the center of the specimen as shown in Fig. 2 (a), many pores were left at the welded joint and caused a welding defect as shown in Photo. 14. To prevent the creation of such pores, as shown in Fig. 2 (b), focus position should be set at the lower side of the specimen. Thus, the inner gas at the bead top would be exhaused and a no-pore welded joint would be obtained as shown in Photos. 12 and 13. Also, to obtain no-pore good welded joint, it would be more effective to drill a

Photo. 14 View of pore at welded zone, 150 kv, 11 mA, 1000 mm/min, a_b*=0.95, 18% porosity

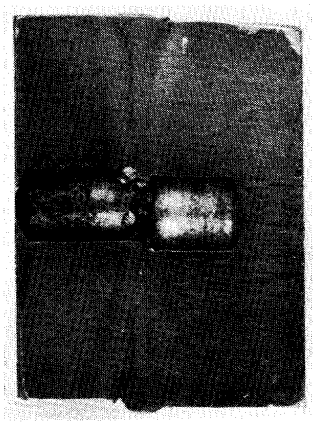

Photo. 15 View of E.B. welded specimen with small hole, 150 kv, 11 mA, 1000 mm/min, a_b*=0.95, 10% porosity

small hole at the center of specimen as shown in Fig. 2 (c). Then, a no-pore welded joint would be easily obtained as shown in Photo. 15. However, in the case of Fig. 2 (d), both sides of the specimen, that is, the entrance side, and the exist side of the beam were melted down and the welded area was greatly reduced with bad result. Also, when the welding operation was carried out at a low welding speed, the width of the welded zone was enlraged and the volume of generated gas was increased, therefore, the pore creation at the welded jeint was promoted. Photo. 16 shows a view of the pores at the welded zone.

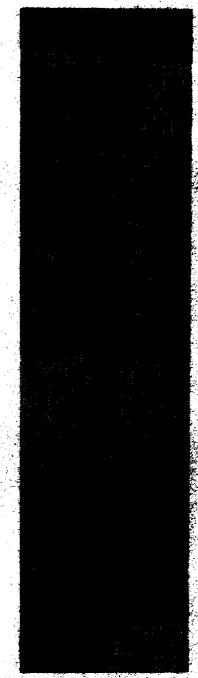

Photo. 16 View of pores at welded zone (welding speed: 600 mm/min), 150 kv, 7 mA, a_b^*=0.86, 14% porosity

3.2 *Shrinkage of weld zone*

As above mentioned, in the electron beam welding of sintered metal, it was observed that the beam penetrated zone of sintered metal had shrunk compared with the apparent volume of unwelded structure because of the fusing of the sintered structure and turning into the solid state structure. The relation between the beam power (accelerating voltage × beam current) and the shrinkage of the specimens with each porosity is shown in Figs. 5 and 6. The measurement of the shrinkage of the speeimens was carried out by measuring the difference in the length of the two abutted specimens before and after the welding operation. From the two figures, it is seen that the shrinkage of the welded specimens increases with the beam power or the heating quantity. Also, concerning the relation between the porosity and the shrinkage, it is clear that the shrinkage of the specimen increases with an increase of porosity. In addition, as to the relation between the accelerating voltage and the shrinkage, there is observed a tendency that under the constant beam power, the shrinkage of the welded specimen decreases with an increase of the accelerating voltage

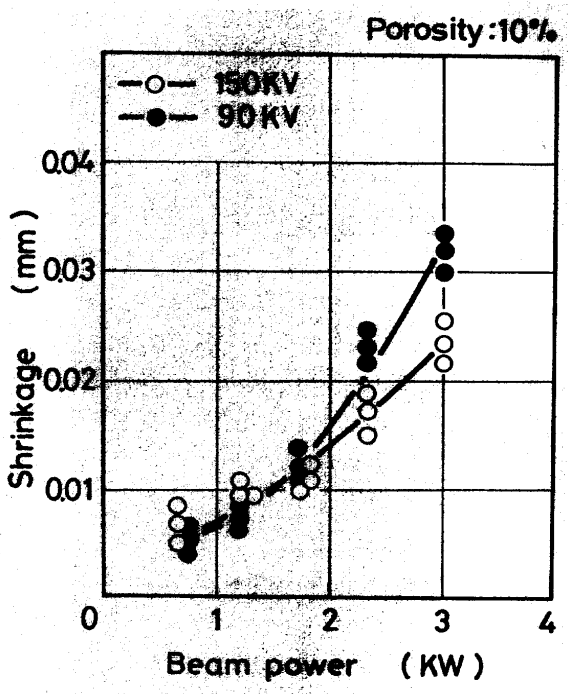

Fig. 5 Relation between beam power and shrinkage (porosity: 10%)

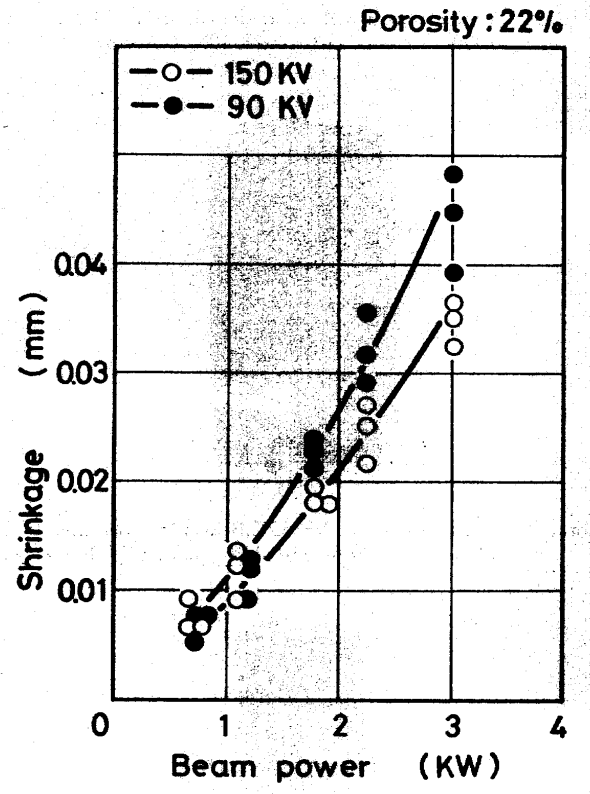

Fig. 6 Relation between beam power and shrinkage (porosity: 22%)

because of the reduction of the beam diameter and the width of the fused zone. However, this tendency is not extreme. Fig. 7 shows the relation between the shrinkage of specimen and the porosity for each accelerating voltage. From this figure, it is clearly seen that the shrinkage of each specimen increases with an increase of porosity.

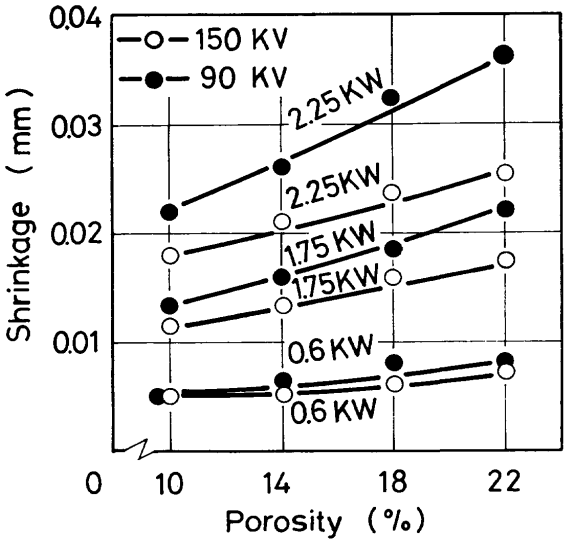

Fig. 7 Relation between porosity and shrinkage

3.3 *Hardness distribution of welded joint*

The hardness distribution of the specimen welded by electron beam welding is shown in Fig. 8. From this figure, it is clearly seen that the hardness of sintered metals depends on the porosity, and the hardness of a specimen with low porosity is higher than that of one with high porosity. Also, the hardness of the fused zone is higher than that of the non-fused zone because of the structure of the fused zone being the same as that of the solid metal. Photo. 17 shows a view of the tested specimen.

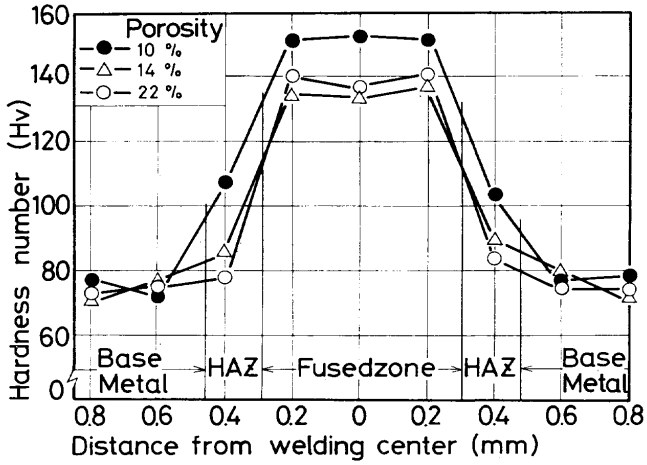

Fig. 8 Hardness distribution of E.B. welded specimen

Conclusions

The conclusions obtained in this experiment are summarized as follows:

(1) The pores in the sintered iron which the electron beam had penetrated, disappeared and a solid state developed when the sintered structure had been melted by the beam current. And the difference between the structure of the welded zone and that of the base sintered iron was clearly observed.

(2) It was observed that several cracks which caused a lowering of the welding strength, initiated at the boundary of the welded zone owing to the high porosity of the sintered iron or due to the high beam current.

(3) The penetrating depth of the beam current increased with an increased beam current and accelerating voltage, and with an increased porosity of sintered iron.

(4) The penetrating width of the specimen was enlarged with an increased beam current, but concerning the accelerating voltage, the reverse tendencies were observed because of the electron beam diameter being reduced with an increased accelerating voltage.

(5) It was observed that some porosities which caused a lowering of the welding strength initiated at the melted zone owing to insufficiency of gas exhaustion.

(6) In order to prevent the pore from developing at the welded zone, it is very important to place the focus position at the lower side of the specimen or use a specimen having a small hooe at the center to facilitate gas exhaustion from the welded zone.

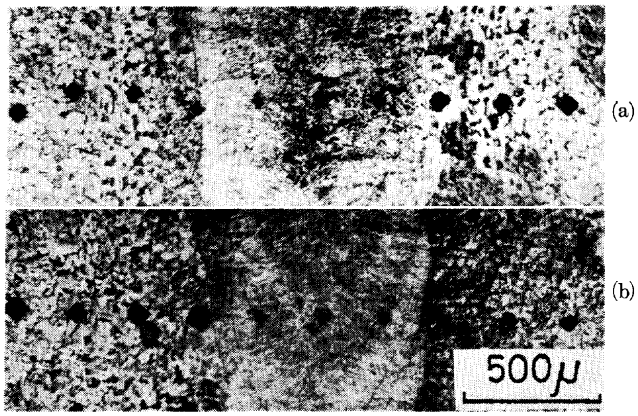

Photo. 17 Hardness distribution of E.B. welded sintered iron. (a): 10% porosity (b): 22% porosity, 150 kv, 11 mA, 1000 mm/min, $a_b^*=0.86$

References

1) W.V. Knoop: "Joining of P/M Structure' S.A.E. Journal, 740984 (1974).
2) J.E. Hinrichs, P.W. Ramsey and M.W. Zimmermann: Welding Journal, p. 242 (1971).
3) I. Onishi: "Arc Welding of Sintered Iron" The Precision Machine Vol. 32, No. 2, p. 724–727 (1966).